



Sliding mode control technique to regulate DC/DC buck converters in systems exploiting photovoltaic power generation

Le Tien Phong, Nguyen Thi Thanh Thuy

Electrical Faculty, Thai Nguyen University of Technology, Thai Nguyen, Vietnam

Abstract

This paper introduces a new method, called IB-SMC method, to control DC/DC buck converters in systems exploiting photovoltaic power generation. This method combines the iterative-bisectional technique in the maximum power point tracker and the sliding mode control technique to adjust operational modes of photovoltaic power generation. The IB-SMC controller uses a voltage sliding surface to evaluate the relation between the value of instantaneous voltage at the input terminal of the DC/DC converter and the value of instantaneous voltage at the maximum power point. Using information about the power of electromagnetic radiation from a pyranometer and temperature from a temperature sensor, the sliding surface and hysteresis band are modified by practically operational conditions that help improve energy efficiency of the process exploiting photovoltaic power generation. Simulations are carried out by Matlab/Simulink that show the ability to ensure dynamic stability by tracking instantaneous maximum power point at any time whenever having any change of the operational condition, static stability by maintaining the operational point at maximum power point whenever not having any change of the operational condition and help bring out approximately absolute energy efficiency.

Keywords: equivalent control signal, maximum power point, maximum power point tracker, photovoltaic power generation, sliding mode control, sliding surface

1. Introduction

The development of photovoltaic power generation (PVg) has helped this generation become a potential source to replace traditional sources. All studies about PVg mainly focus on exploiting it in isolated or grid-connected systems. As other renewable source, the main factors affecting to be able to generate power of PVg are parameters of operational conditions, namely: the power of electromagnetic radiation (G), temperature of p-n junction (T) and load. Commercial productions of PVg are often verified under the standard test condition (STC) that has $G=1000\text{W/m}^2$ and $T=25^\circ\text{C}$. Due to the variation of input energy, the operational condition at any time is specified by a pair-value (G, T). Due to the relationship between the output power and the absorbed ability of load, it is often exploited through power converters. Therefore, controllers play an important role in regulating control pulse to adjust a suitable load corresponding to the power at the maximum power point (MPP).

A modern control technique which has been applied in systems exploiting PVg is the sliding mode control (SMC) technique. To use the SMC technique, a sliding surface must be chosen to achieve a destination. Applied in systems exploiting PVg, power or voltage sliding surfaces are often used in two approaches to reach MPP.

For the first approach, controllers considered the SMC technique as a maximum power point tracker (MPPT) [1, 2]. It didn't correctly evaluate the essence of PVg because they considered its load impedance as a constant. This approach could be only used in some cases because the inductor and

capacitor in DC/DC converters couldn't fully adapt to the change of operational conditions.

For the second approach, the SMC technique could be combined with a technique to determine MPP in MPPT such as P&O (perturb and observe) or ESC (extremum seeking control) technique. In this approach, controllers always actively seek a new operational point due to unknown the variation of G and T, therefore they still has the same disadvantages of P&O or ESC technique [3-9]. They make power loss and can't exploit all energy from PVg.

The above analysis shows that the way to control power converter needs to change to achieve the purpose of exploiting maximum available energy from PVg. Particularly, the information about MPP must be accurately determined before providing as a destination to the controller. A technique proposed to determine MPP recently, called the IB (iterative and bisectional) technique, can accurately provide parameters at MPP under any operational condition by using a pyranometer (PYR) to measure G and a temperature sensor (TempS) to measure T. The IB technique helps to calculate instantaneous values of V_{mpp} or P_{mpp} at MPP which is sent to the controller to create a suitable control pulse. In this case, the controller interferes to the power circuit of power converters to drive the current operational point to the desired point (MPP).

This paper proposes a new method combining the IB technique and the SMC technique to regulate a DC/DC buck converter. Section II will introduce the mathematical description of the DC/DC buck converter, the IB technique

and the SMC technique. Equivalent control signal and stable analysis will be represented in in section III. Section IV will show simulation results and comments and the last section will represent some conclusions.

2. Structural system and mathematical model

2.1 Structural system

The structural system to exploit PVg is described in Fig. 1.

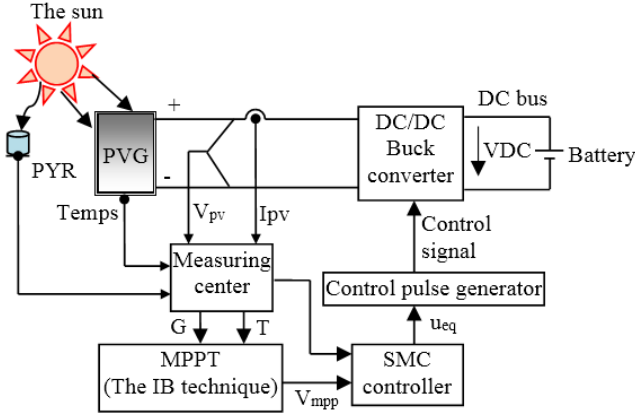


Fig 1: The structural system

The measuring center collects the information about G from the PYR, T from the Temps, value of v_{pv} and i_{pv} from voltage and current sensors placed at the output terminals of PVg.

The SMC controller calculates the equivalent control signal (u_{eq}) which is provided to the control pulse generator to create control signal before sending to a controlled switch (SW) placed in the DC/DC buck converter.

The operational states of PVg are specified by two main parameters which are G and T . In the practical operation, G and T always continuously change that make operational points move away from real MPPs. Therefore, MPPT needs to use the IB technique to accurately calculate parameters at instantaneous MPP. Value of V_{mpp} determined by MPPT must be provided to the SMC controller and considered as a destination for the controller under any operational condition. Combining the IB technique and the SMC technique, a new control method is constructed to regulate operational modes for PVg, called IB-SMC method.

2.2 Modeling the DC/DC buck converter

Power circuit of a DC/DC buck converter is described in Fig. 2a including a SW and storage elements (L , C) which are capable of charging or discharging energy. Equivalent circuits of this converter corresponding to on and off states of SW are depicted in Fig. 2b and Fig. 2c [10].

Where:

R_{dc} , L_{dc} are resistance and inductance of the inductor placed in the converter.

C_{pv} , C_{dc} are the capacitance of capacitors at the PVg side and the DCbus side.

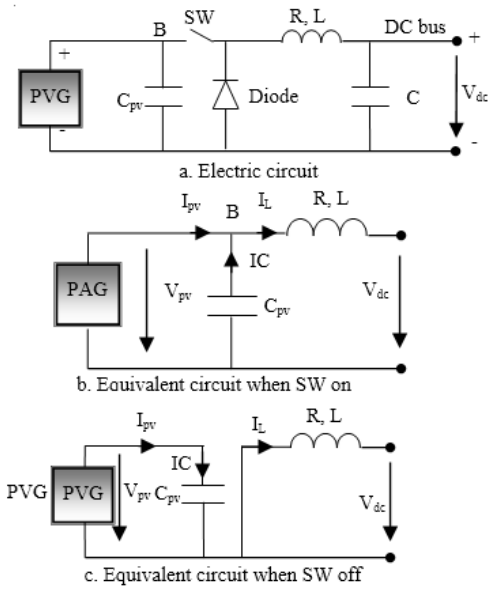


Fig 2: Power circuit and equivalent circuits corresponding to on and off states of SW

Apply the Kirchoff's first and second laws for the circuit corresponding to the on and off states of SW, we have equations (1) and (2) [13]:

$$L \frac{di_L}{dt} = v_{pv} u - V_{dc} \quad (1)$$

$$i_C = i_{pv} - i_L u \quad (2)$$

2.3 Modeling PVg

Equivalent circuit of PVg is described in Fig. 3 [11].

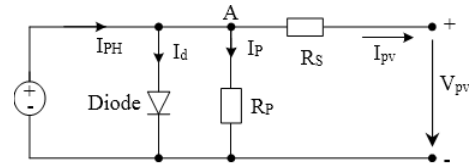


Fig 3: Equivalent circuit of PVg

The relationship between current i_{pv} and voltage v_{pv} at output terminals of PVg is defined by (3):

$$i_{pv} = I_{ph} - I_0 \left\{ \exp \left(\frac{v_{pv} + i_{pv} R_s}{n V_t} \right) - 1 \right\} - \frac{v_{pv} + i_{pv} R_s}{R_p} \quad (3)$$

Output power from PVg is defined by (4):

$$p_{pv} = v_{pv} i_{pv} \quad (4)$$

Where: R_s is series resistor; R_p is parallel resistor; I_0 is reserve saturation current; I_{ph} is photo-generated current; V_t is thermal voltage at p-n junctions; n is ideality factor.

2.4 Description of MPPT

The IB technique is proposed basing on accurately mathematical model of PVg to have pair-value (V_{mpp} , I_{mpp}) corresponding to the peak of the v_{pv} - p_{pv} curve which is set by a value-pair (G, T). By combining the iterative technique and bisectional technique, MPPT calculates and observe the power value of three continuous points to evaluate the moving statement of operating points. The IB technique is represented in Fig. 4 [11].

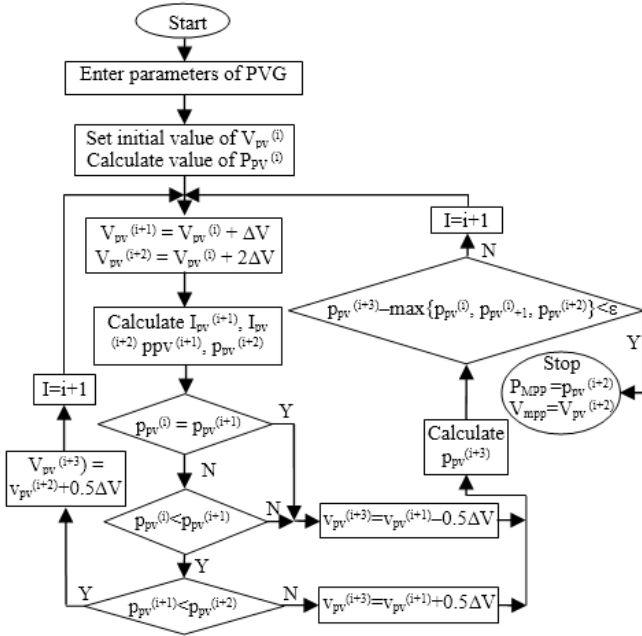


Fig 4: The IB technique to determine MPP

3. The IB-SMC Method

3.1 State system of equations

Rewrite (1) and (2) equations, we have the state system of equations:

$$\begin{cases} \dot{x}_1 = -\frac{V_{dc}}{L_{dc}} - \frac{R_{dc}}{L_{dc}}x_1 + \frac{x_2}{L_{dc}}u \\ \dot{x}_2 = \frac{i_{pv}}{C_{pv}} - \frac{x_1}{C_{pv}}u \end{cases} \quad (5)$$

Where: $x = [x_1 \ x_2] = [i_L \ v_{pv}]$ is the state vector,

$$f(x) = \begin{bmatrix} -\frac{V_{dc}}{L_{dc}} - \frac{R_{dc}}{L_{dc}}x_1 \\ \frac{i_{pv}}{C_{pv}} \end{bmatrix}$$

is drift vector,

$$g(x) = \begin{bmatrix} \frac{x_2}{L_{dc}} \\ -\frac{x_1}{C_{pv}} \end{bmatrix}$$

is control vector.

3.2 Sliding surface

To control DC/DC buck converter, sliding surface is defined by a function as depicted in (6) or (7):

$$h = x_2 i_{pv} - P_{mpp} + K_a i_C = 0 \quad (6)$$

or

$$h = x_2 i_{pv} - P_{mpp} + K_a (i_{pv} - x_1) = 0 \quad (7)$$

Where:

P_{mpp} is the value of power at MPP which must be reached (the result of the IB technique and considered as a constant at the considered time corresponding to a pair-value (G, T)),

i_{pv} is the function of variable x_2 ($i_{pv} = i_{pv}(x_2)$),

K_a (V/A) is the quantity which evaluates the relative sliding speed between power and current. Value of K_a affects to the chattering phenomenon (vibration of v_{pv} around V_{mpp}) in the SMC technique [3].

3.3 Stable analysis

The time derivative of the sliding surface is defined by (8):

$$\begin{aligned} \frac{dh}{dt} &= \frac{d [x_2 i_{pv} - P_{mpp} + K_a (i_{pv} - x_1)]}{dt} \\ \Leftrightarrow \dot{h} &= x_2 \frac{di_{pv}}{dx_2} \dot{x}_2 + i_{pv} \dot{x}_2 + K_a \frac{di_{pv}}{dx_2} \dot{x}_2 - K_a \dot{x}_1 \end{aligned} \quad (8)$$

According to Lyapunov's theory, (9) must be always suitable to exist stably around the sliding surface [12, 13]:

$$\begin{cases} \lim_{h \rightarrow 0^-} \frac{dh}{dt} \Big|_{u=1} = \frac{dh}{dt} \Big|_{u=1, h=0} > 0 \\ \lim_{h \rightarrow 0^+} \frac{dh}{dt} \Big|_{u=0} = \frac{dh}{dt} \Big|_{u=0, h=0} < 0 \end{cases} \quad (9)$$

Using (8) and (9), we have boundaries to limit the stable area in the process of sliding the current operational point to a new operational point:

$$\begin{cases} A \left(\frac{i_{pv}}{C_{pv}} - \frac{x_1}{C_{pv}} \right) - K_a \left(-\frac{V_{dc}}{L_{dc}} - \frac{R_{dc}}{L_{dc}} x_1 + \frac{x_2}{L_{dc}} \right) > 0 \\ A \frac{i_{pv}}{C_{pv}} - K_a \left(-\frac{V_{dc}}{L_{dc}} - \frac{R_{dc}}{L_{dc}} x_1 \right) < 0 \end{cases} \quad (10)$$

where,

$$A = \frac{di_{pv}}{dx_2} x_2 + \frac{di_{pv}}{dx_2} K_a + i_{pv}$$

3.4 Equivalent control signal

Equivalent control signal u_{eq} is the equivalence between the extremely high switching frequency of the control signal (0, 1) and the smooth control signal. Therefore, u_{eq} is a smooth feedback control law to maintain the orbit of ideal state that is always bounded on the surface S when the initial state of system $x(t_0)=x_0$ is also on the surface S or $h(x_0)=0$ [12].

The derivative of function h in the direction $f(x)$ is

$$L_f h = \frac{\partial h}{\partial x^T} f(x) \quad \text{and the derivative of function } h \text{ in the direction}$$

$$g(x) \text{ is } L_g h = \frac{\partial h}{\partial x^T} g(x). \quad L_{gh} \text{ and } L_{fh} \text{ are defined by (11) and (12):}$$

$$L_g h = \frac{\partial h}{\partial x^T} g(x) = \begin{bmatrix} -K_a & i_{pv} + x_1 & \frac{\partial i_{pv}}{\partial x_2} \end{bmatrix} \begin{bmatrix} \frac{x_2}{L_{dc}} \\ -\frac{x_1}{C_{pv}} \end{bmatrix}$$

$$\Leftrightarrow L_g h = -K_a \frac{x_2}{L_{dc}} - \frac{x_1}{C_{pv}} \left(i_{pv} + x_1 \frac{\partial i_{pv}}{\partial x_2} \right) \quad (11)$$

$$L_f h = \frac{\partial h}{\partial x^T} f(x) = \begin{bmatrix} -K_a & i_{pv} + x_1 & \frac{\partial i_{pv}}{\partial x_2} \end{bmatrix} \begin{bmatrix} -\frac{V_{dc}}{L_{dc}} - \frac{R_{dc}}{L_{dc}} x_1 \\ \frac{i_{pv}}{C_{pv}} \end{bmatrix}$$

$$\Leftrightarrow L_f h = K_a \left(\frac{V_{dc}}{L_{dc}} + \frac{R_{dc}}{L_{dc}} x_1 \right) + \frac{i_{pv}}{C_{pv}} \left(i_{pv} + x_1 \frac{\partial i_{pv}}{\partial x_2} \right) \quad (12)$$

From (11) and (12), u_{eq} ($0 < u_{eq} < 1$) is defined by (13):

$$u_{eq} = \frac{\frac{i_{pv}}{C_{pv}} \left(i_{pv} + x_1 \frac{\partial i_{pv}}{\partial x_2} \right) + K_a \left(\frac{V_{dc}}{L_{dc}} + \frac{R_{dc}}{L_{dc}} x_1 \right)}{\frac{x_1}{C_{pv}} \left(i_{pv} + x_1 \frac{\partial i_{pv}}{\partial x_2} \right) + K_a \frac{x_2}{L_{dc}}} \quad (13)$$

3.5 Control strategy

Control strategy for IB-SMC method is reprinted in Fig. 5.

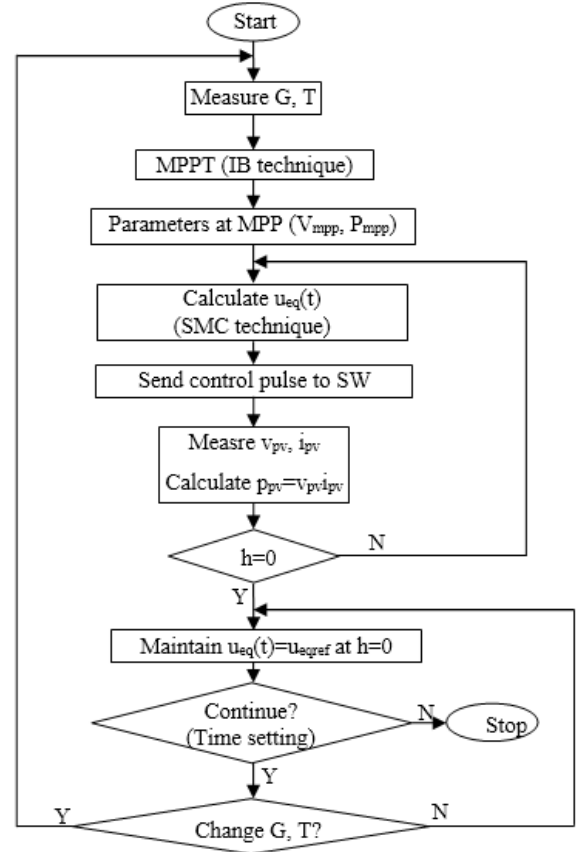


Fig 5: Control strategy for the IB-SMC method

4. Simulation

4.1 Simulation parameters

Simulation parameters of the power converter, DCbus and switching frequency are represented in Table 1. Parameters of PVg are represented in Table 2. Function $n(T)$ is defined by (14).

Table 1: Parameters of power converter, DCbus, switching frequency

	Symbol	Value
DC/DC buck converter	R (Ω)	0.5
	L (H)	8.10^{-3}
	C (F)	10^{-3}
Voltage at DCbus	V_{dc} (V)	12
Switching frequency	f_s (kHz)	50

$$n(T) = 1 - 0.008017 \Delta T + \frac{9}{400000} \Delta T^2 \quad (14)$$

Where, $\Delta T = T - 25^\circ\text{C}$.

Table 2: Parameters of PVg under the stc

Parameters	Value
Short-circuit current(A)	7.36
Open-circuit voltage (V)	30.4
Voltage at MPP (V)	24.2
Current at MPP (A)	6.83
Current coefficient by T (%/°C)	0.057
Voltage coefficient by T (%/°C)	-0.346
Power coefficient by T (%/°C)	-0.478
Photo-generated current (A)	7.3616
Reverse saturation current (A)	$1.03 \cdot 10^{-7}$
Thermal voltage at p-n junctions (V)	1.6814
Series resistor (Ω)	0.2511
Parallel resistor (Ω)	1172.1

Received energy in range time (0:t) is defined by (15) and energy efficiency is defined by (16):

$$A(t) = \int_0^t p_{pv}(t) dt \quad (15)$$

$$H\% = \frac{A(t)}{A_{mpp}} 100\% \quad (16)$$

4.2 Simulation results

To evaluate the effect of K_b to the hysteresis band and chattering phenomenon when using the SMC technique, the energy efficiency is considered in case $K_b = -0.05$ (as a constant) and in case $K_a = -0.05 * G / G_{stc}$ (change by G). Values of T are given with discrete values of 25°C , 35°C , 45°C , 55°C , 65°C . Simulation time is 1s corresponding to three levels $G = 1000\text{W}/\text{m}^2$, $G = 600\text{W}/\text{m}^2$ and $G = 200\text{W}/\text{m}^2$. Simulation results are represented in Fig. 6, Fig. 7, Fig. 8.

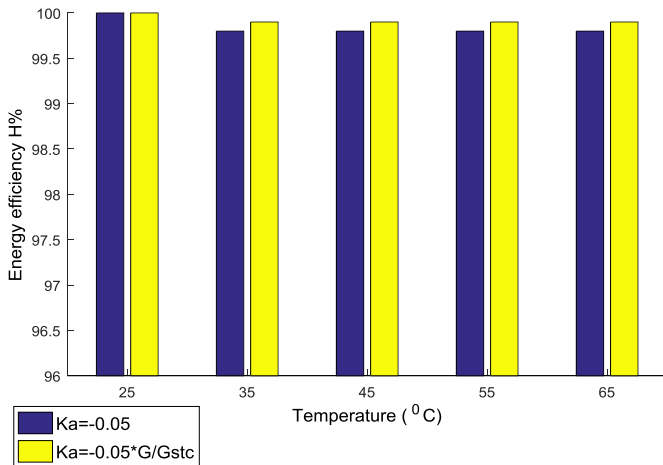


Fig 6: Energy efficiency corresponding to $G = 1000\text{W}/\text{m}^2$

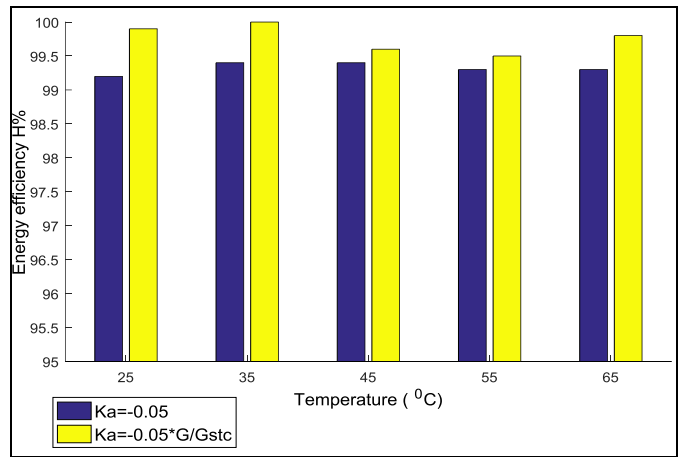


Fig 7: Energy efficiency corresponding to $G = 600\text{W}/\text{m}^2$

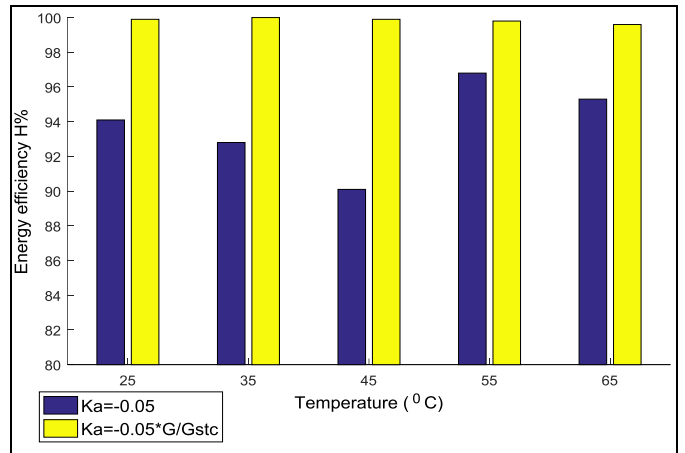


Fig 8: Energy efficiency corresponding to $G = 200\text{W}/\text{m}^2$

Simulation results obtained in Fig. 6, Fig. 7, Fig. 8 showed that the energy efficiency decreased when K_a didn't change whereas it always approximately achieved 100% corresponding to changing K_a by G. It means that the IB-SMC method with the irradiance dependence of K_a can help exploit maximum available energy from PVg due to making the hysteresis band smaller and decreasing the chattering phenomenon as described in Fig. 9. Because of this, the IB-SMC method is also considered as an adaptive method under any operational condition.

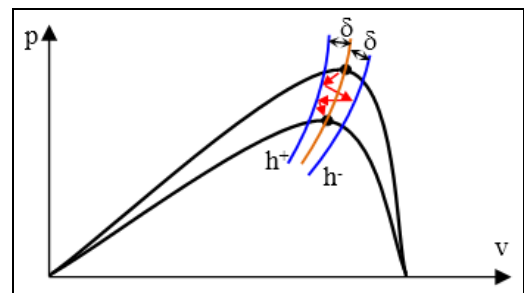


Fig 9: The movement of operational points in the v-i plane

To evaluate the ability to track MPP, a scenario to operate PVg is considered in case $T = 40^\circ\text{C}$ and the variation of G in 3 seconds as depicted in Fig. 10.

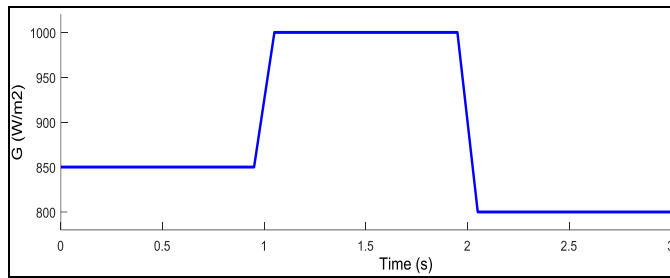


Fig 10: The variation of G

The instantaneous power characteristic about $p_{pv}(t)$, $P_{mpp}(t)$ and $A(t)$ energy characteristic in three seconds are represented in Fig. 11.

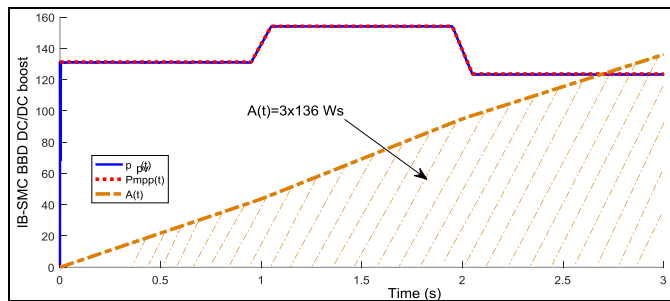


Fig 11: p_{pv} , P_{mpp} , $A(t)$ characteristic

Current through the C_{pv} capacitor is represented in Fig. 12.

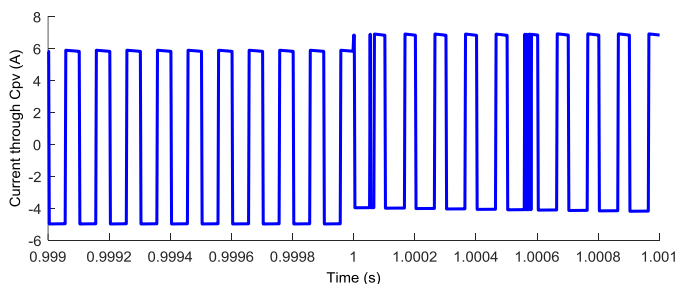


Fig 12: Current through the C_{pv} capacitor at the 1st second

Energy efficiency corresponding to the scenario is defined by (17):

$$H \% = \frac{3 \times 136}{408.7} 100 \% = 99.83 \% \quad (17)$$

Simulation results show that the $p_{pv}(t)$ characteristic always accurately tracks the $P_{mpp}(t)$ characteristic at the time of unchanging G (ensure static stability) or at the time of increasing or decreasing G (ensure dynamic stability) in whole process of operating PVg. Therefore, the IB-SMC method helps to almost completely exploit energy of PVg at all times. With the simulation results of the i_c current in Fig. 13, it has a form of a alternative current in triangular waveforms and very small amplitude. Because of having small amplitude of i_c , coefficient K_c in the sliding surface does not affect much to the chattering phenomenon, so it doesn't need to correct it by G.

6. Conclusion

This paper proposes a new method combining the IB technique and the SMC technique to exploit PVg. Because of using the IB technique in MPPT, the IB-SMC method becomes an effective methodology to ensure static and dynamic stability in the process of operating PVg. It also provides a different approach to exploit maximum available energy under any operational condition.

To apply the SMC technique to regulate the DC/DC buck converter, parameters in the sliding surface affect much to hysteresis band, chattering phenomenon, stable ability of the system. Due to accurately describing the performance of PVg, these parameters can be determined through simulation process to evaluate prior to practical application by the survey of all operational conditions (G or T varies in typical ranges).

Due to using a PYR and a TempS, instantaneous information about MPP is determined and considered as a desired destination for the controller. They help to modify the sliding surface and the hysteresis band according to the practically operational conditions, therefore the IB-SMC method is considered as an adaptive control method. Until now, they have many types and become more popularly because of more suitable cost. It shows the ability to apply the IB technique in practical applications. Otherwise, to measure the current through the C_{pv} capacitor, it needs to use small loss transformers and frequency of measuring devices must be higher several times than frequency of i_c . These problems can be overcome by using high technical solutions but the cost of whole system increase very much. This makes the IB-SMC method difficult to become popular.

7. References

1. Fan Zhang, Jon Maddy, Giuliano Premier, Alan Guwy. Novel current sensing photovoltaic maximum power point tracking based on sliding mode control strategy, *Solar Energy*, 2015, 118(41).
2. Ramesh M, Sanjeeva Rayudu S, Polu Raju R. A New Approach to Solve Power Balancing Problem in Grid Coupled PV System using Slide Mode Control, *Indian Journal of Science and Technology*. 2015; 8(17):57. ISSN (Online): 0974-5645.
3. Daniel Gonz'alez Montoya, Carlos Andres Ramos Paja, Roberto Giral. Improved design of sliding mode controllers based on the requirements of MPPT techniques, *IEEE Transactions on Power Electronics*, 2015.
4. Emil A Jimenez Brea, Eduardo I Ortiz-Rivera. Simple Photovoltaic Solar Cell Dynamic Sliding Mode Controlled Maximum Power Point Tracker for Battery Charging Applications, *Applied Power Electronics Conference and Exposition (APEC)*, 25th Annual IEEE, 2010, (40).
5. Gaga Ahmed, Errahimi Fatima, ES-Sbai Jania. Design and Simulation of a Solar Regulator Based on DC-DC Converters Using a Robust Sliding Mode Controller, *Journal of Energy and Power Engineering*, David Publishing, 2015, 9(44).

6. Omar Boukli-Hacene. Robust Regulation of the Photovoltaic Voltage using Sliding Mode Control as Part of a MPPT Algorithm, *International Journal of Computer Applications*, 0975-8887. 2013; 78(11):(74).
7. Oswaldo Lopez-Santos. Contribution to the DC-AC conversion in photovoltaic systems: Module oriented converters, Thesis for Philosophy Doctor degree, Institut National des Sciences Appliquées de Toulouse (INSA de Toulouse) in Automation, 2015, (75).
8. Reham Haroun, Abdelali El Aroudi, Angel Cid-Pastor, Germain Garica, Carlos Olalla, Luis Martinez-Salamero. Impedance Matching in Photovoltaic Systems Using Cascaded Boost Converters and Sliding-Mode Control, *IEEE Transactions on Power Electronics*. 2015; 30(6):(85)
9. Yoash Levron, Doron Shmilovitz. Maximum Power Point Tracking Employing Sliding Mode Control, *IEEE Transactions on Circuits and Systems*. 2013; 60(3):103.
10. Siew-Chong Tan, Yuk-Ming Lai, Chi Kong Tse. Sliding Mode Control of Switching Power Converters – Techniques and Implementation, *CRC Press*, Taylor and Francis Group, 2012.
11. Le Tien Phong, Ngo Duc Minh, Nguyen Van Lien. A New Method to Identify Maximum Power Point for Photovoltaic Generation, *IEEE ComManTel Conference placed in Viet Nam and IEEEExplore*, 2015. ISBN: 978-1-4673-6547-5.
12. Hebertt Sira-Ramirez, Ramon Silva-Ortigoza. Control Design Techniques in Power Electronics Devices, Springer Publisher, 2006. e-ISBN 1-84628-459-7,
13. Siew-Chong Tan, Yuk-Ming Lai, Chi Kong Tse. Sliding Mode Control of Switching Power Converters – Techniques and Implementation, *CRC Press*, Taylor and Francis Group, 2012.